Relativistic MHD simulations of Pulsar Wind Nebulae

Luca Del Zanna

Gruppo Plasmi Astrofisici
http://www.astro.unifi.it/gruppi/plasmi/

Dipartimento di Astronomia e Scienza dello Spazio - Università di Firenze

In collaboration with: Elena Amato, Niccolò Bucciantini, Delia Volpi

---

Outline

- Numerical simulations in high-energy astrophysics
  - The relativistic MHD equations
  - Shock-capturing numerical schemes
  - A central-type code for RMHD: methods and tests
- Pulsar Wind Nebulae in Supernova Remnants
  - Observations
  - Models (analytical, numerical)
- The inner jet-torus structure (e.g. Crab Nebula)
  - Observations
  - Theoretical background
  - 2-D axisymmetric RMHD simulations
  - Synchrotron emission and comparison with observations
- Summary and conclusions

Why numerical simulations?

Relativistic flows and shocks in high-energy astrophysics:

- Active Galactic Nuclei
- Compact X-ray sources
- Gamma-Ray Bursts
- Pulsar Wind Nebulae

Problem: 3-D dynamics of relativistic plasmas

Solution: shock-capturing codes for relativistic MHD

Relativistic MHD equations

- Covariant form (fluid eqs. + Maxwell eqs. + freeze-in):

$$\nabla_\mu (\rho u^\mu) = 0$$

$$\nabla_\mu [(w + b^2) u^\mu u^\nu - b^\mu b^\nu + (p + b^2/2) g^{\mu\nu}] = 0$$

$$\nabla_\mu (u^\mu b^\nu - u^\nu b^\mu) = 0$$

- where (c=1, 4π→1):

$$x^\mu = (t, x^j),\ \ u^\mu = (\gamma, \gamma v^j),\ \ b^\mu = (\gamma v_i B^i, B^j/\gamma + \gamma v_i B^i v^j)$$

$$\gamma = (1 - v_i v^i)^{-1/2},\ w = e + p,\ \ e = \rho + p/(\Gamma - 1)$$

In the following we shall consider special relativity

Shock-capturing numerical schemes

Any set of hyperbolic conservation laws

$$\frac{\partial U}{\partial t}+\sum_{i=1}^{n}\frac{\partial F^{i}(U)}{\partial x^{i}}=0$$

may be solved by high-order Godunov schemes:

- grid discretization (finite volumes or differences)
- reconstruction of U and F at intercells (TVD, ENO)
- approximate Riemann solver for fluxes (upwind step)
- time integration (two-steps or higher order RK)

Problem: MHD and RMHD systems are not strictly hyperbolic

The divergence-free condition

The equation for the B field yields, as in classical MHD:

$$\nabla\cdot\mathbf{B}=0,\quad \partial_t\mathbf{B}=\nabla\times(\mathbf{v}\times\mathbf{B})$$

the specific operator structure (a curl) in the induction equation must be considered to preserve the constraint

We use the Upwind Constrained Transport method for MHD (UCT: *Londrillo & Del Zanna, ApJ 2000; JCP 2004)*

- CT staggered discretization (*Evans & Hawley, 1988*)
- staggered B components in fluxes (to avoid monopoles)
- four-state numerical magnetic fluxes

A simple and efficient central-type scheme

- from point-value conservative to primitive variables
- third-order Convex ENO (CENO3) reconstruction at intercells of right and left values (component-wise)
- central-type HLL or LLF averaged solvers:

$$F^{\mathrm{HLL}} = \frac{\alpha^+ F^{\mathrm{L}} + \alpha^- F^{\mathrm{R}} - \alpha^+\alpha^-(U^{\mathrm{R}} - U^{\mathrm{L}})}{\alpha^+ + \alpha^-}, \quad F^{\mathrm{LLF}} = \frac{1}{2}[F^{\mathrm{L}} + F^{\mathrm{R}} - \alpha(U^{\mathrm{R}} - U^{\mathrm{L}})]$$

$$\alpha^\pm = \max\{0, \pm\lambda^\pm_{\mathrm{L}}, \pm\lambda^\pm_{\mathrm{R}}\}, \quad \alpha = \max\{\alpha^+, \alpha^-\}$$

- from numerical fluxes to spatial derivatives
- iteration for each spatial direction, iteration in time (RK)

Spectral decomposition and Riemann solvers not required!

From classic MHD to relativistic MHD

- Ubiquitous presence of Lorentz factor in the equations implies numerical derivation of primitive variables from conservative ones (a 5x5 nonlinear system that can be reduced to a single root-finding by projecting along B)
- Magnetosonic speeds are derived from a quartic equation
- Eigenvectors are more complex (but not needed here!)
- Independent reconstruction of vector components may prevent simulations with ultra-relativistic speeds or magnetic fields. In these cases we might even use the global LF with $\alpha = 1$
- Papers: *Del Zanna & Bucciantini, 2002; Del Zanna et al., 2003*

Numerical tests: hydrodynamics

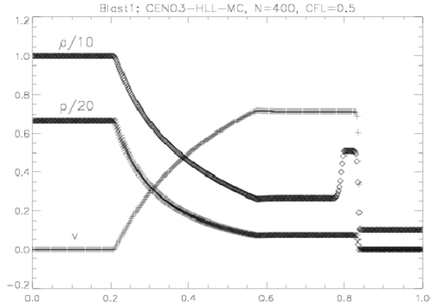

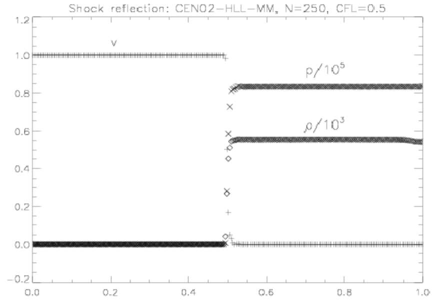

- Blast wave

$(\rho, v, p)^L = (10,0,13.3)$

$(\rho, v, p)^R = (1,0,10^{-6})$

$t = 0.4$

- Shock reflection

$(\rho, v, p) = (1,0.99999,0.01)$

$t = 0.75$

Numerical tests: magnetohydrodynamics

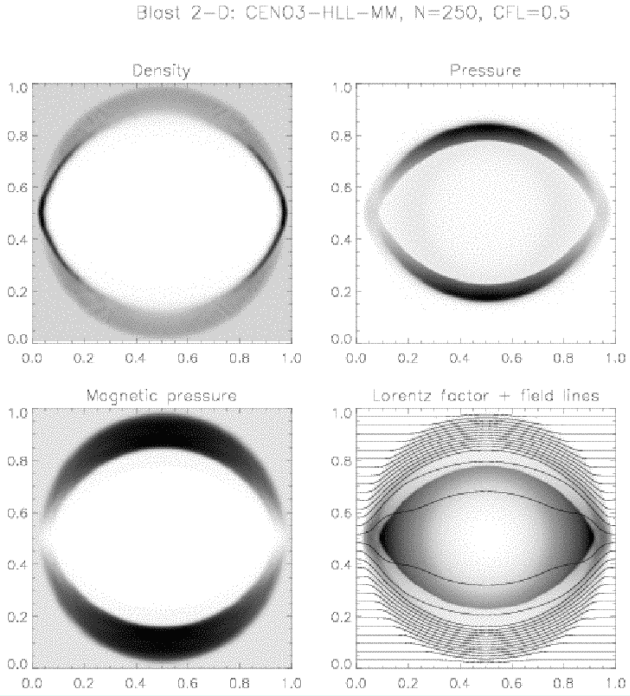

- MHD 2-D blast wave

$(\rho, p, B_x) =$

$(1,10^3, 4), r \leq 0.08$

$(1,10^{-2},4), r > 0.08$

$t = 0.4$

Numerical tests: axisymmetric relativistic jet

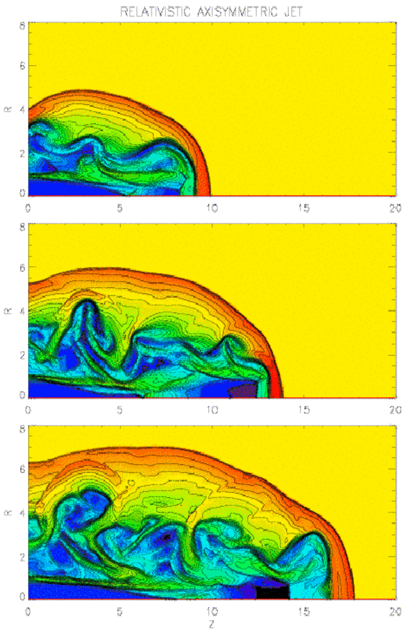

$$(\rho, v_z, v_r, p) = (0.1, 0.99, 0, 0.01),\ r \le 1, z \le 1$$

$$(\rho, v_z, v_r, p) = (10, 0, 0, 0.01),\ r > 1, z > 1$$

$$M \approx 18 \qquad 0 \le t \le 40$$

Pulsar Wind Nebulae

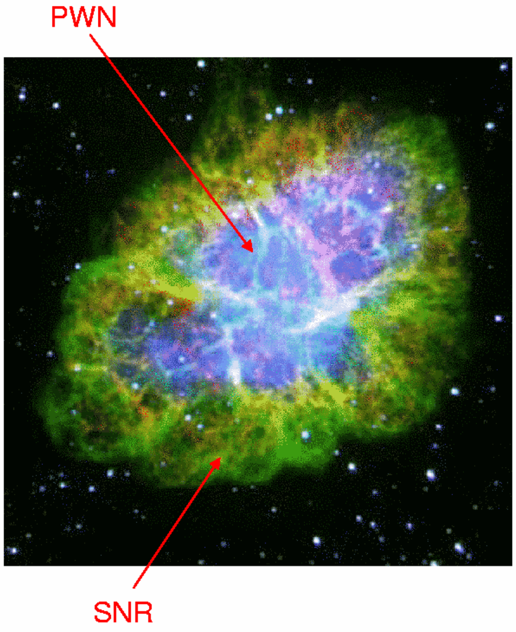

- PWNe are hot bubbles (plerions) emitting non-thermal radiation (synchrotron) at all wavelengths: require injection of relativistic particles and magnetic fields
- Originated by the interaction of the ultra-relativistic magnetized pulsar wind with the expanding SNR dense ejecta
- Crab Nebula in optical: central amorphous mass (continuum) + external filaments (lines)

Sketch of PWN / SNR interaction

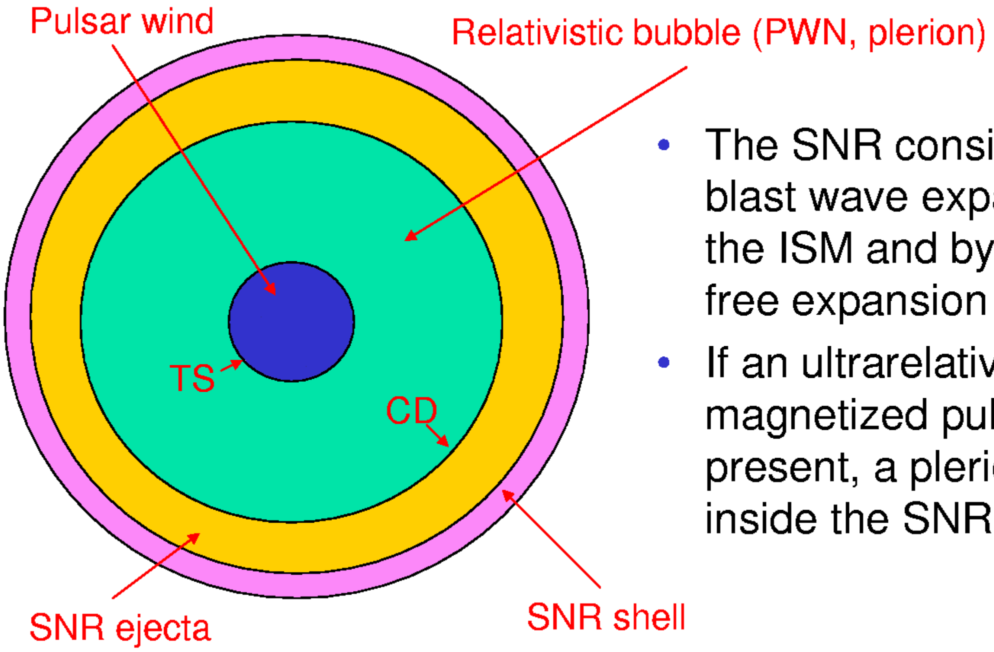

- The SNR consists of a blast wave expanding in the ISM and by ejecta in free expansion
- If an ultrarelativistic and magnetized pulsar wind is present, a plerion forms inside the SNR

Pulsar magnetosphere and wind

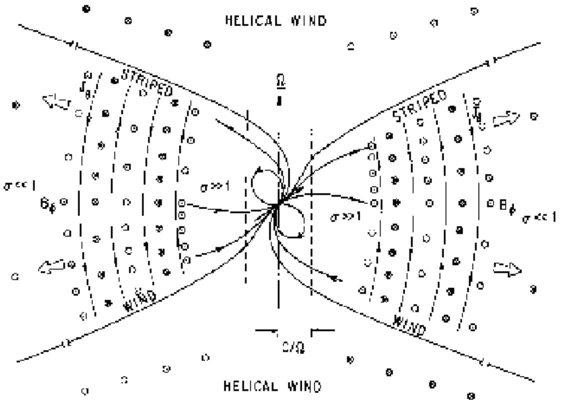

- Pulsar spin-down energy is converted to Poynting flux (mainly a toroidal field) and in a pair wind (with $\sigma >> 1$)
- At the TS models predict $\sigma << 1$ to match the observed synchrotron emission: the *sigma paradox*!
- *Striped wind*: the magnetic field may decrease because of equatorial reconnection or dissipation of fast waves at TS

PWNe analytical MHD theory (KC84)

- PWN theory is mainly based on 1-D analytic (*Rees & Gunn 1974; Kennel & Coroniti, 1984*) and self-similar (*Emmering & Chevalier, 1987*) MHD models
- KC84 (spherically symmetric, stationary):
  - assume that the wind terminates with a strong MHD shock
  - solve the relativistic jump conditions at TS
  - solve the equations in the PWN region
  - calculate the synchrotron emission
  - a best fit analysis provides the wind parameters:

$$R_{TS} = 3\times10^{17}\,cm, \quad L = 5\times10^{38}\,erg/s, \quad \gamma = 3\times10^{6}, \quad \sigma = 3\times10^{-3}$$

PWNe and SNRs: 1-D RHD simulations

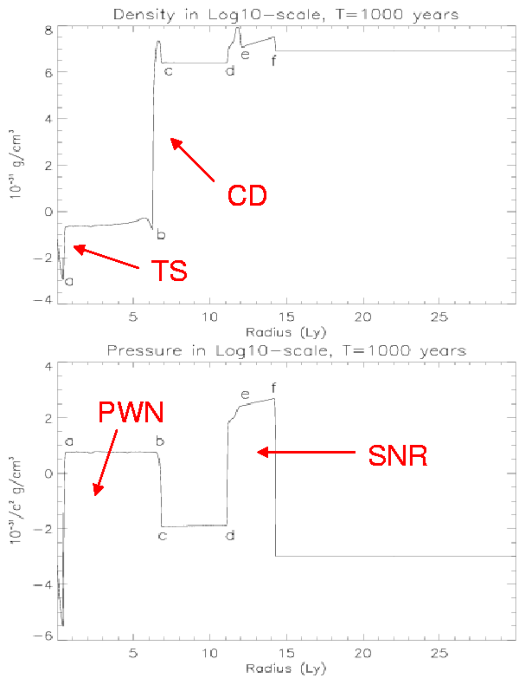

- a: wind termination shock
- b: PWN-SNR contact discontinuity
- c: shell of swept up ejecta
- d: reverse shock
- e: SNR-ISM contact discontinuity
- f: SNR blast wave

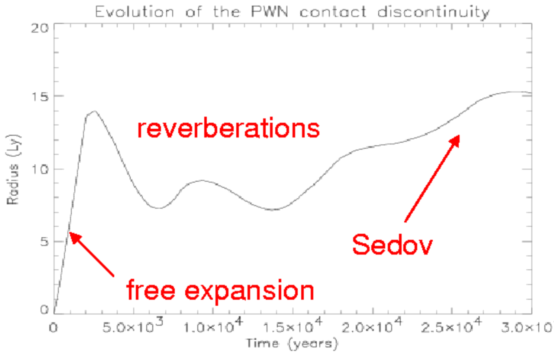

PWNe and SNRs: 1-D RMHD simulations

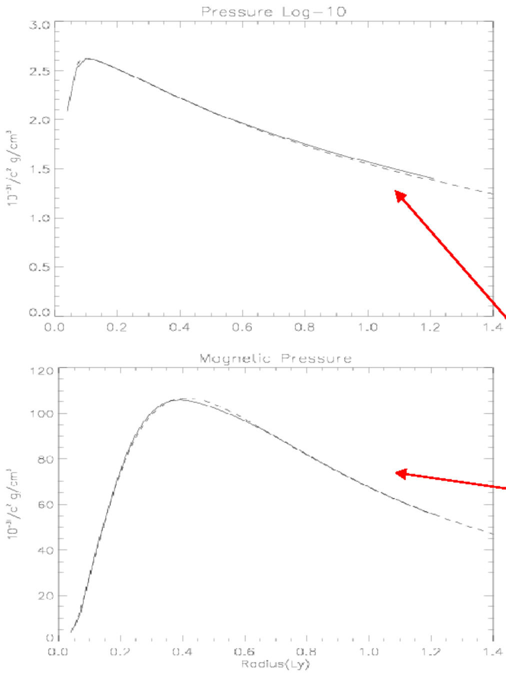

- Addition of a toroidal B
  - Equipartition reached in PWN
  - TS moves closer to the pulsar
  - CD evolution driven by the total pressure at CD radius: $E \approx 4\pi R_{pwn}^3 P_{tot}(R_{pwn})$
- Comparison with RMHD self-similar models
  - Thermal pressure
  - Magnetic pressure
- Papers on 1-D RMHD:
  - *Bucciantini et al. 2003; 2004*

Jet-torus structure: Chandra X-ray images

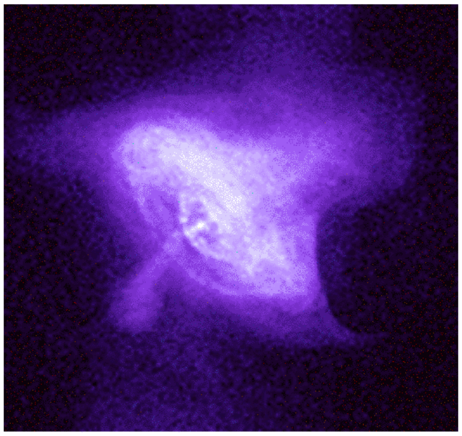

Crab

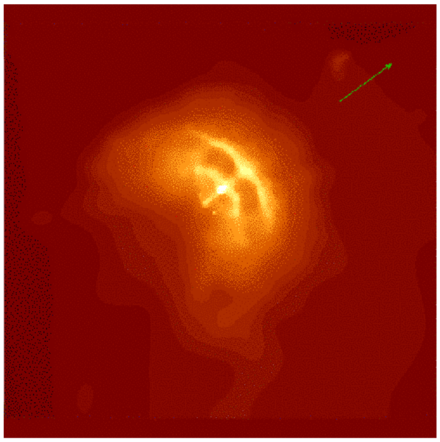

Vela

- Crab nebula (*Weisskopf et al., 2000; Hester et al., 2002*)
- Vela pulsar (*Helfand et al., 2001; Pavlov et al., 2003*)
- Other objects: PSR 1509-58, G0.9+01, G54.1+0.3

Jet-torus structure: Chandra X-ray movies

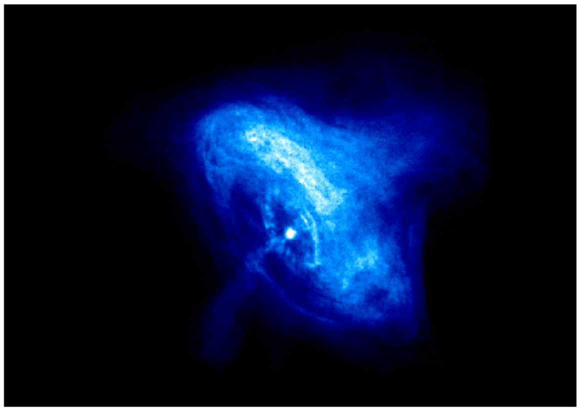

Crab

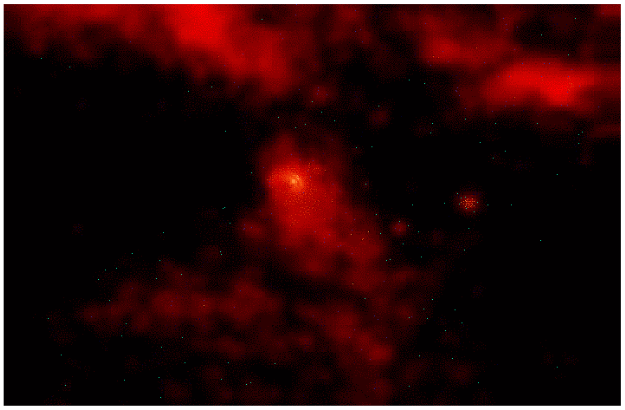

Vela

- Equatorial motions (wisps): v=0.3-0.5 c
- Polar jet motions: v=0.5-0.8 c

Jet-torus structure: theory

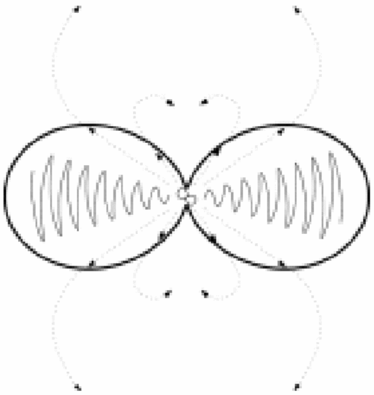

- Torus: higher equatorial energy flux?
- Jets: magnetic collimation?

$$\gamma >> 1 \Rightarrow \rho_q \vec{E} + \vec{j} \times \vec{B} \approx 0$$

collimation downstream of the TS?

  - *Bogovalov & Khangoulian, 2002*
  - *Lyubarsky, 2002*

- Axisymmetric RMHD simulations of the interaction of an anisotropic relativistic magnetized wind with SN ejecta
  - *Komissarov & Lyubarsky, 2003*
  - *Del Zanna, Amato & Bucciantini, 2004*

Axisymmetric relativistic wind model

- Far from the pulsar light cylinder the wind is expected to be ultrarelativistic, cold, and weakly magnetized. We assume:
  - Isotropic mass flux, anisotropic energy flux $(F \propto \rho\gamma^2)$:

$$\rho(r,\theta) = \rho_0 (r_0/r)^2 \gamma_0/\gamma(\theta), \quad \gamma(\theta) = \gamma_0[\alpha + (1-\alpha)\sin^2(\theta)]$$

  - Purely toroidal magnetic field:

$$B(r,\theta) = B_0 (r_0/r)\sin(\theta)$$

  - Parameters of the wind model:

$$\gamma_0 >> 1,\ \alpha = \frac{F(r_0,0)}{F(r_0,\pi/2)} << 1,\ \ \sigma = \frac{B_0{}^2}{4\pi c^2 \rho_0 \gamma_0^2} << 1$$

Simulation setup

- Central-type conservative RMHD code (here second order)
- Spherical geometry, axial symmetry (r,θ)
- Poloidal velocity and purely toroidal magnetic field
- Computational grid: 400 points in r, 100 in θ
- Boundaries: injection for r=0.05 ly, extrapolation for r=20 ly
- Long time simulations (beginning of reverberation phase)
- High accuracy near the center: extremely small timesteps!
- Initial conditions:
  - Pulsar ultrarelativistic wind
  - Spherical shell of expanding dense ejecta
  - Static unmagnetized ISM

PWN self-similar evolution and TS shape

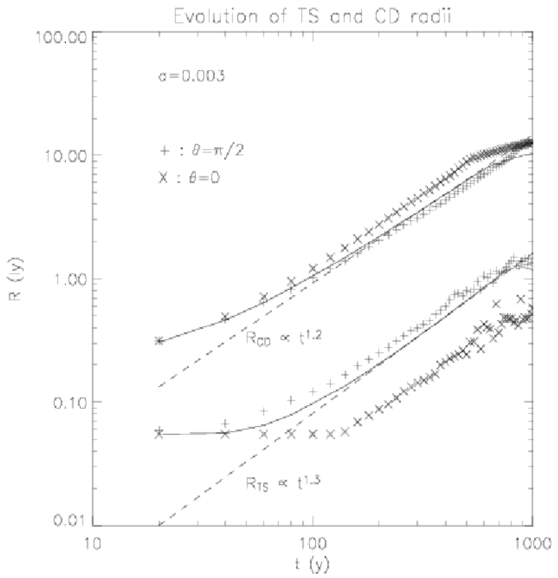

- Expected TS profile:

$$R(\theta) \approx R_0\sqrt{\alpha+(1-\alpha)\sin^2(\theta)}$$

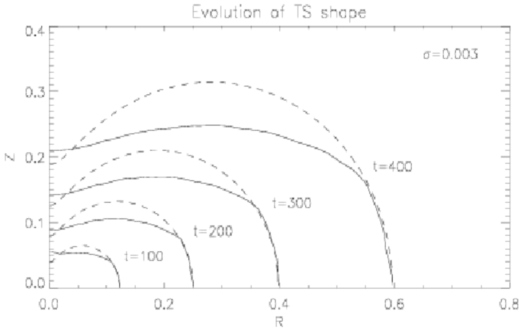

$$\gamma_0 = 100,\ \alpha = 0.1,\ \sigma = 0.003$$

PWN elongation

- Magnetic pinching effect (*Begelman & Li, 1992*):

$$\frac{\partial}{\partial z}\left(\frac{B^2}{8\pi}+P\right) \approx 0,\quad \frac{\partial}{\partial r}\left(\frac{B^2}{8\pi}+P\right) \approx -\frac{B^2}{4\pi r}$$

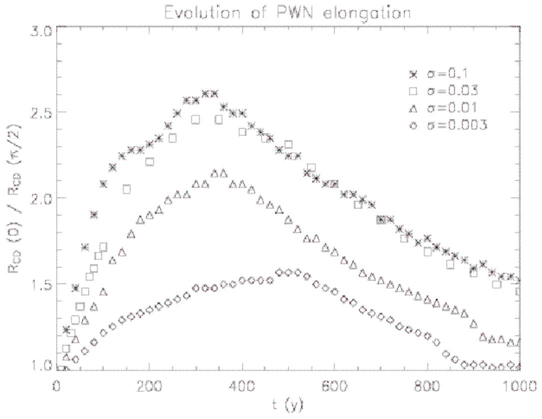

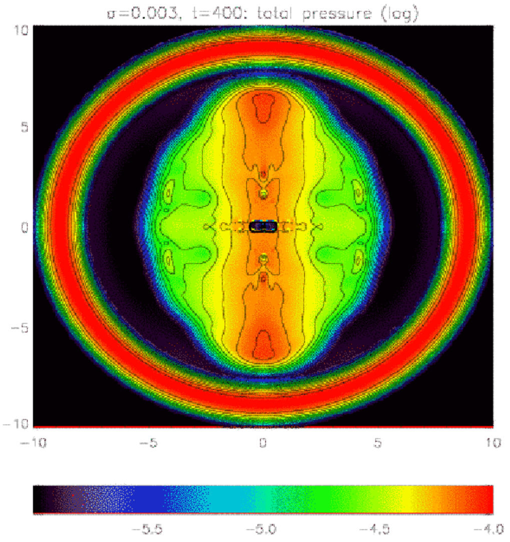

TS structure and flow pattern

- The wind anisotropy shapes the TS structure. A complex flow pattern arises:
  - A: ultrarelativistic pulsar wind
  - B: subsonic equatorial outflow
  - C: supersonic equatorial funnel
  - D: super-fastmagnetosonic flow
  - a: termination shock front
  - b: rim shock
  - c: fastmagnetosonic surface

σ=0.003

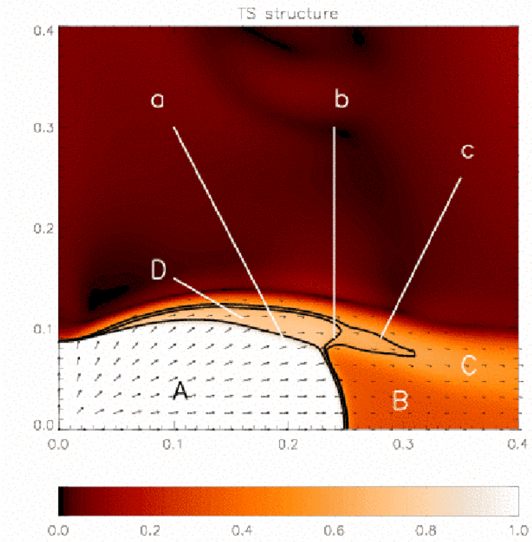

Formation of polar jets by hoop stresses

- The flow pattern changes drastically with increasing σ
- For high magnetization (σ>0.01) a supersonic jet is formed

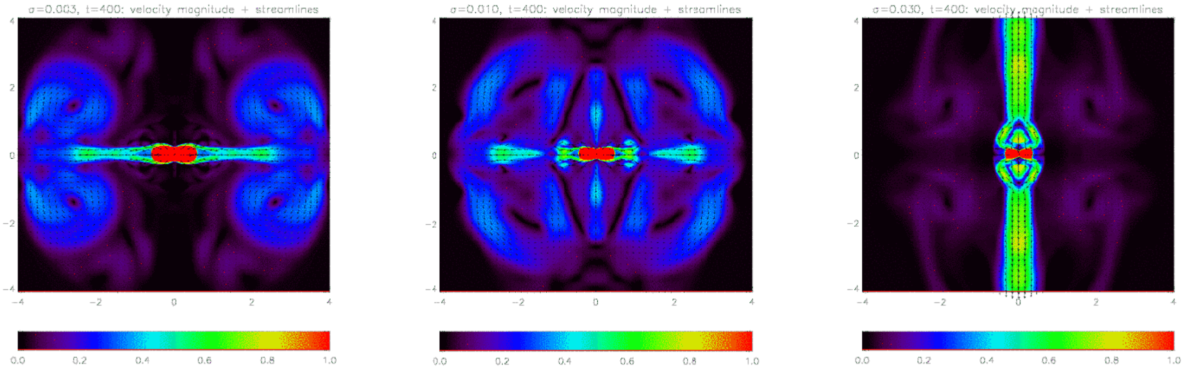
σ=0.003 σ=0.01 σ=0.03

PWN crunching by instabilities at CD

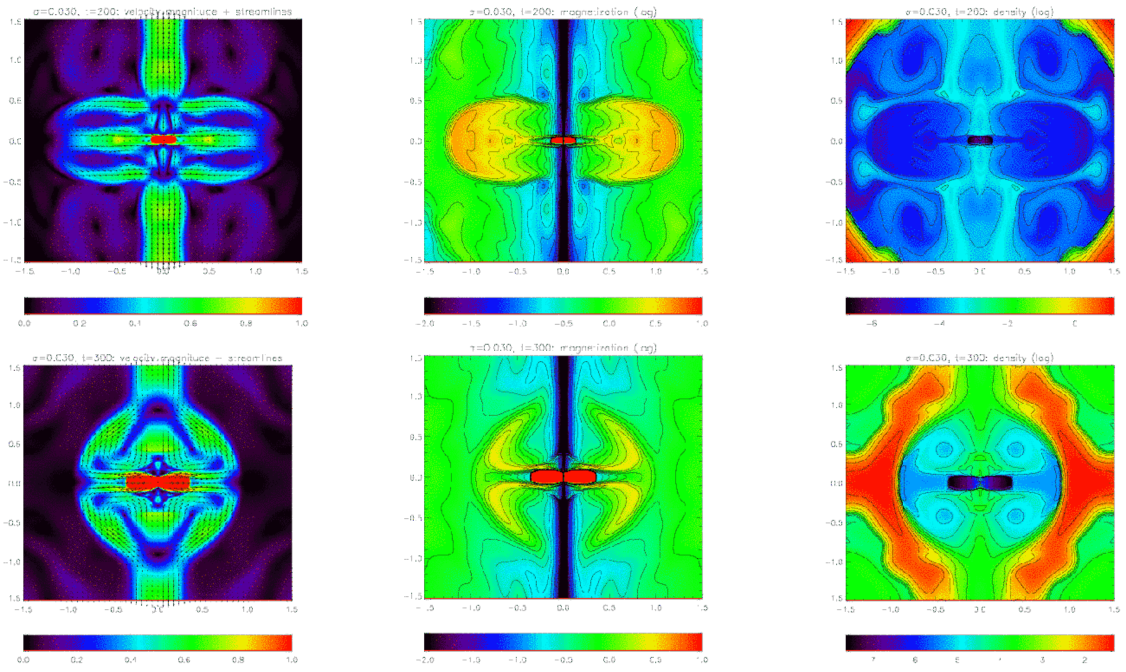

Dependence on the field shape

- Initial magnetic field with a narrow equatorial neutral sheet

$$B(r,\theta) = B_0\left(\frac{r_0}{r}\right)\sin(\theta)\ \tanh[b(\pi/2-\theta)]$$

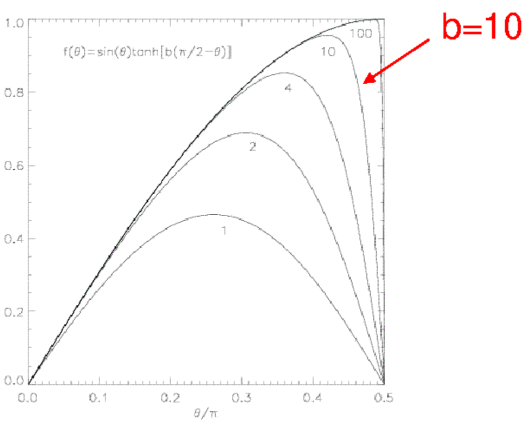

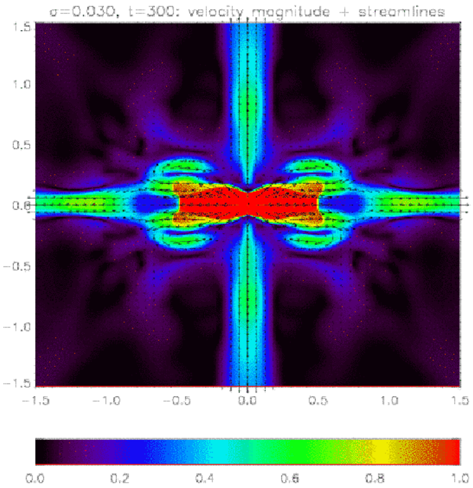

Comparison with observations

- Synchrotron emission maps:
  - Assume a power law spectrum of electron energies at TS

$$f_0(\varepsilon_0) \propto p_0 \varepsilon_0^{-(2\alpha+1)}$$

  - Evolve the energy considering adiabatic and synchrotron losses

$$\frac{d\varepsilon}{dt'} = \varepsilon \frac{d}{dt'} \ln(n^{1/3}) - \frac{4e^4}{9m^3c^5}(B')^2 \varepsilon^2$$

  - Assume emission at the critical frequency

$$\nu \propto B_\perp' \varepsilon^2$$

  - Calculate the spectral emissivity function in the observer frame

$$j_\nu \propto p\, D^{2+\alpha} (B'_\perp)^{\alpha+1} [1 - \varepsilon(\nu)/\varepsilon_\infty]^{2\alpha-1} \nu^{-\alpha}$$

  - Produce synthethic maps by integrating along the LOS

Comparison with observations

- Simulated synchrotron map vs X-ray Chandra images:

Simulation

$\sigma = 0.03$

$b = 10$

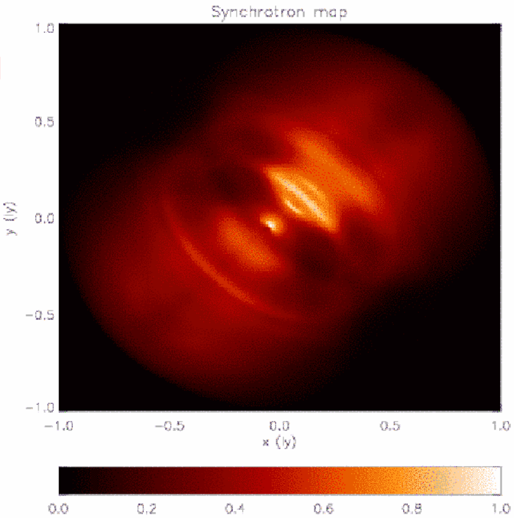

Crab

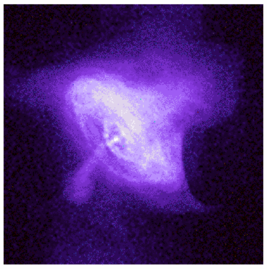

Vela

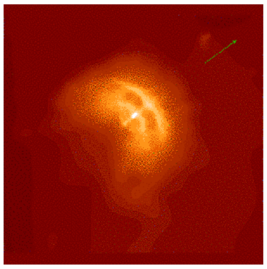

Comparison with observations

- Constraining the field shape:
  - More structures seen when the striped wind region is larger

σ=0.03, b=1

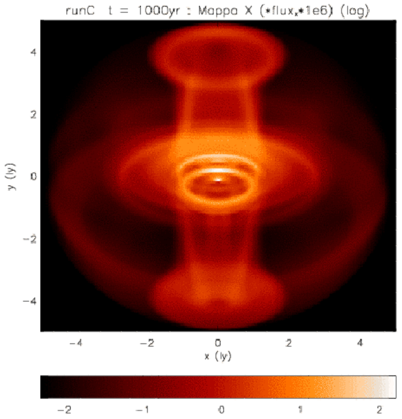

σ=0.03, b=10

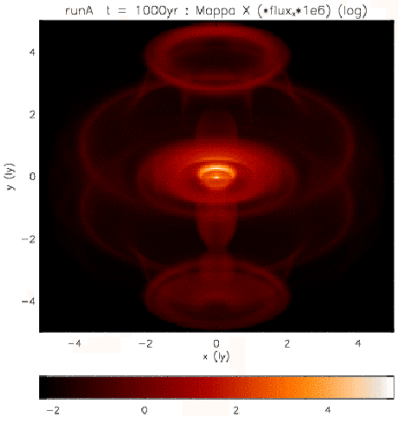

Comparison with observations

- Effects of synchrotron losses: optical vs X-ray maps
  - Runs with realistic L, without ejecta (to avoid crunching)

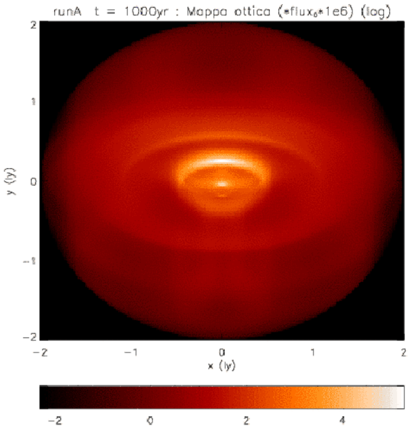

Optical

X-ray

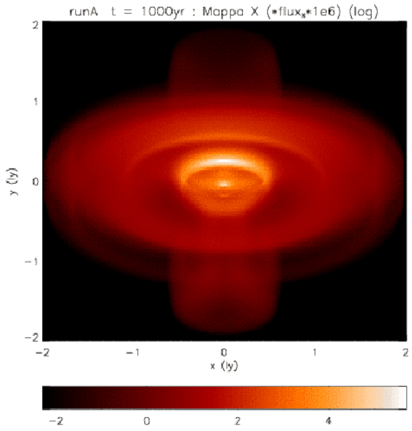

Comparison with observations

- Simulated integrated spectra:
  - Reasonable results for higher magnetization
  - Still problems to get the right spectral break

σ=0.03, b=1

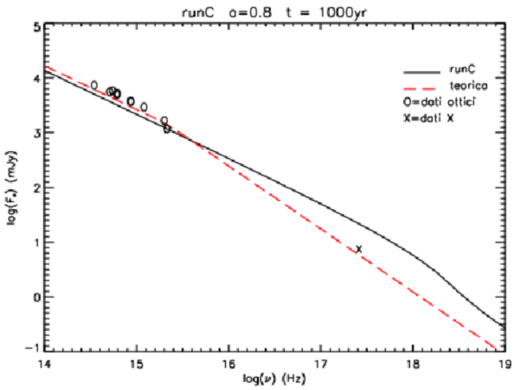

σ=0.03, b=10

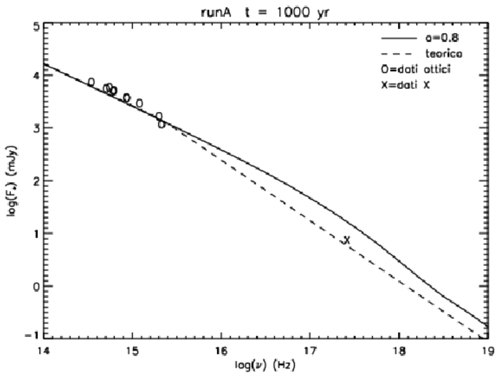

Comparison with observations

- Simulated polarization maps
  - We are waiting for the observational counterpart!

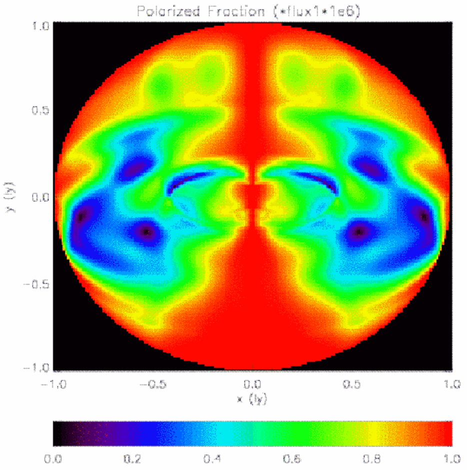

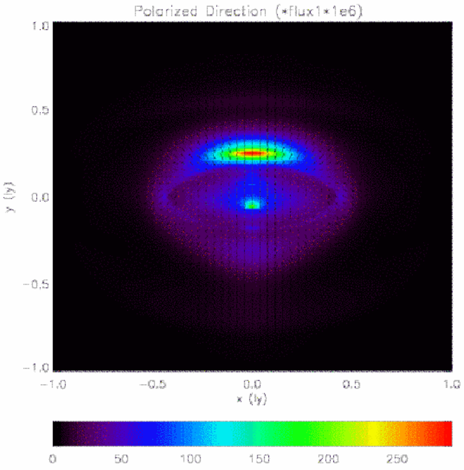

Summary and conclusions

- Many PWNe show a jet-torus structure (Crab, Vela, …)
- The torus is explained with a higher equatorial energy flux
- Jet collimation forbidden in the wind. Inside PWN?
- RMHD axisymmetric simulations confirm this scenario:
  - The TS has a toroidal shape, a strong equatorial flow is produced
  - For $\sigma>0.01$ hoop stresses divert the flow toward the axis
  - Plasma is compressed and a polar jet with $v=0.5$-$0.7c$ is launched
  - CD instabilities driven by large vortexes may crunch the PWN
  - Simulated synchrotron maps resemble closely X-ray images
  - Work in progress: constraining B, spectra and polarization maps

Thank you